Photodynamic Therapy of Nodular Basal Cell Carcinoma with Multifiber Contact Light Delivery

Marcelo Soto Thompson,[1,2] *Stefan Andersson-Engels,*[1,2] *Sune Svanberg,*[1,2] *T. Johansson,*[3] *Sara Pålsson,*[1,2,4] *Niels Bendsoe,*[2,5] *A. Derjabo,*[6] *J. Kapostins,*[6] *Unne Stenram,*[7,2] *J. Spigulis,*[8] *& Katarina Svanberg*[9,2,*]

[1]Department of Physics, Lund Institute of Technology, Lund, Sweden; [2]Lund University Medical Laser Centre, Lund, Sweden; [3]SpectraCure AB, Lund, Sweden; [4]Science and Technology International, Honolulu, HI; [5]Department of Dermatology and Venereology, Lund University Hospital, Lund, Sweden; [6]Latvian Oncology Centre, Riga, Latvia; [7]Department of Pathology, Lund University Hospital, Lund, Sweden; [8]Institute of Atomic Physics and Spectroscopy, University of Latvia, Riga, Latvia; [9]Department of Oncology, Lund University Hospital, SE-221 85 Lund, Sweden

**Corresponding author.* E-mail: Katarina.Svanberg@onk.lu.se

To overcome the limited treatment depth of superficial photodynamic therapy we investigate interstitial light delivery. In the present work the treatment light was delivered using a system in which three or six clear-cut fibers were placed in direct contact with the tumor area. This placement was thought to represent a step toward general purpose interstitial PDT. Twelve nodular basal cell carcinomas were treated employing δ-aminolevulinic acid and 635 nm laser irradiation. Fluorescence measurements were performed monitoring the buildup and subsequent bleaching of the produced sensitizer protoporphyrin IX. The treatment efficacy, judged at a 28-month follow-up, showed a 100% complete response. Two punch excisions at 7 months converted two partial responses to complete responses. One patient failed to appear at all follow-up sessions. The outcome of the treatments was comparable to superficial photodynamic therapy in terms of histological, clinical, and cosmetic results.

KEY WORDS: dosimetry, interstitial, fluorescence, aminolevulinic acid

0731-8898/06/$35.00

Introduction

Photodynamic therapy (PDT) utilizing topical application of δ-aminolevulinic acid (ALA) has been evaluated in the treatment of various malignant and nonmalignant skin lesions.[1–4] For thin lesions, such as superficial basal cell carcinomas (sBCCs), and precancerous conditions in the skin, such as actinic keratoses, the technique seems to gain general acceptance. Clearly, there are several treatment modalities in the management of BCCs. However, ALA-PDT can be considered as the treatment of choice in particular sBCC cases, such as for larger tumor areas and also where other treatment modalities have been performed and failed.[2,4]

ALA-PDT is usually performed utilizing light with a wavelength of 635 nm. At this wavelength the light penetration in tissue is a few millimetres.[5,6] This depth is usually sufficient in the treatment of sBCCs.[7] In thicker tumors, the treatment may give good initial result and healing on the tissue surface, but residual tumor may reside underneath. In order to evaluate the possibility to deliver light more efficiently under such circumstances, interstitial PDT (IPDT) is considered. A number of investigations have been performed employing interstitial light delivery to the tumor.[8–13]

An IPDT system using a multiple fiber arrangement for light delivery has been developed.[14] The input light, to be distributed by the system, comes from a diode laser operating at 635 nm. The treatment fibers could, in principle, also be utilized for measuring the delivered light dose and for monitoring the drug-related fluorescence, the oxygen content in the tissue, and temperature changes during the treatment. The monitoring of these parameters, relevant for light interaction with tissue, is of great importance for adequate light dosimetry.

The aim of the study was to obtain a first evaluation of clinical efficacy and impact of measuring various treatment parameters during PDT of BCCs using our newly developed system, with the multiple fibers mounted in close contact with the treatment area, while not perforating the skin (Fig. 1A). This multifiber contact arrangement consti-

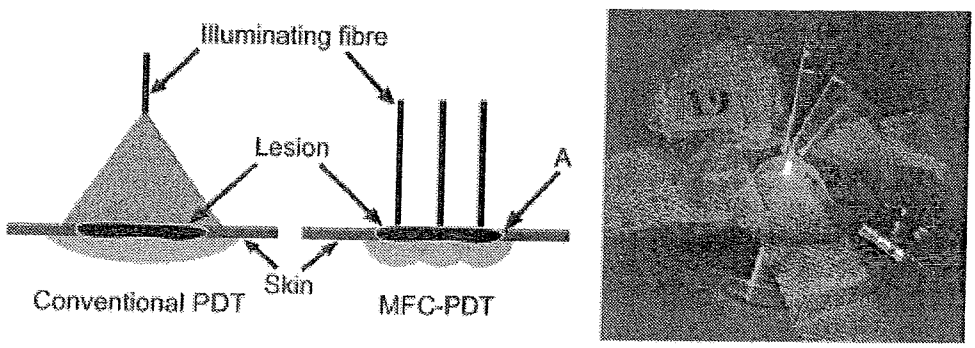

FIGURE 1. (A) Conceptual difference between conventional PDT with superficial illumination (left) and multifiber contact PDT (MFC-PDT) (right). The indicated point **(A)** represents a position in the tumor located far from the treatment fibers. A sufficient dose of treatment light must reach this location after extensive multiple scattering within the tissue. **(B)** Fiber holder setup during tumor treatment, with the aluminum ring attached to the patient.

tutes a valuable development toward IPDT, and possible adverse effects or limitations are more easily monitored. To our knowledge this is the first time this type of multifiber contact PDT (MFC-PDT) with individually planned dosimetry calculations has been clinically performed.

Patients and Methods

Patients

The present study was performed in Riga (Latvia), with approval from the local ethics committee, as an interdisciplinary collaboration between groups in Riga and Lund, comprising oncologists, pathologists, and physicists. Patients referred to the Department of Surgery at the Latvian Oncology Centre, Riga, from general practitioners distributed over Latvia were considered for the study. A punch biopsy was taken from each lesion. After signing a written consent, patients with histopathologically verified nodular BCCs were included in the study and referred to the Oncology Centre for treatment. Tissue biopsies collected for the tumors treated with MFC-PDT were also investigated by a second independent pathologist at the Department of Pathology at the Lund University Hospital. The patients were scheduled for follow-up at 1, 7, and 28 months, at which time the clinical and cosmetic outcomes were assessed, using the criteria described in detail elsewhere.[15]

In total, 10 patients [four male and six female; median age 70 years (29–79 years)] with 12 BCC lesions were treated. More than half of the lesions (8/12) were located on the back of the patients; one lesion was located in the face, and two on the thoracic wall. All lesions exhibited a thickness of 2 mm or more as assessed by palpation and histopathological evaluation. The treatment sessions were conducted as a part of a larger work introducing dermatological use of PDT in Latvia.

Sensitizing Agent

As a tumor sensitizer δ-aminolevulinic acid (ALA, 5-aminolevulinic acid, Batch-No.: M01130 AA, Medac GmbH, Hamburg, Germany) was used. The ALA powder was dissolved in a few drops of physiological saline solution (0.9%) and mixed with an oil-in-water emulsion (Essex Cream, Schering Corp., Kenilworth, NJ) to a concentration by weight of 20% ALA. The preparation of the tumor area and adjacent surrounding skin was done by cleansing it with 70% ethanol. The treatment area, including a margin of ~ 10 mm outside the visible tumor borders, was topically applied with the ALA-containing cream. A plastic film (Tegaderm™, 3M, Loughborough, UK) was applied to maintain the cream in position. A layer of a cotton-based medical coverage (Mefix®, SCA Mölnlycke, Sweden) was then attached to the area as a light-protecting shield. The ALA was applied for 4–6 hr before the irradiation procedure was initiated.

Fluorescence Measurements

The kinetics of the ALA-induced PpIX was monitored by using a clinically adapted, point monitoring fluorosensor (details of the system are presented below). The measurement followed a scheme that previously has been described.[16,17] Briefly, the diagnostic

measurements were performed at seven different times during the whole treatment procedure. First the autofluorescence from normal skin constituents was recorded, serving as a reference for following measurements made at 1, 2, and 4 hr after the application of the ALA cream. Measurements were also performed in connection with the PDT procedure: before, immediately after, and 1 hr after PDT. With this scheme, we were able to follow the buildup, the photodegradation due to the therapeutic treatment, as well as the regeneration of the PpIX after the treatment. Occasionally, because of practical reasons, some of the measurements were not conducted in all patients; this especially applies for the measurement 1 hr after the treatment.

At each time the sites measured were located 10, 5, and 2 mm outside of the visible tumor border, as well as at the tumor border and at the tumor center. For lesions of a diameter larger than approximately 8–10 mm, a position also 2 mm inside the tumor border was measured. At every location an average was formed by measuring three points at the same relative distance to the tumor while moving the fiber slightly between each measurement. This was done to avoid possible local bleaching of the PpIX by the measurement itself and to reduce intrapatient variations. During every measurement the site was prepared by temporarily (for ~ 3 min) removing the dressing and excess ALA cream.

The fluorescence monitoring system consisted of a fiber-based optical multichannel analyzer.[18] The excitation wavelength used was 405 nm with a pulse length of ~ 3 ns and a pulse energy of ~ 10 μJ, achieved with a nitrogen laser pumped-dye laser system (VSL 337 and DLM 220, respectively; Laser Science Inc., Cambridge, MA). The excitation light was focused via a 50% beam splitter onto the proximal tip of a 600 μm core low-fluorescent quartz fiber. When measuring, the distal tip of the fiber was held in gentle contact to the tissue and the induced fluorescence was then guided back through the fiber, deflected by the beam splitter, and focused onto the entrance slit of a spectrometer (MS 125, Oriel Corp., Stratford, CT) The fluorescence spectrum (200–800 nm, 2.2 nm resolution FWHM) was recorded on a thermoelectrically cooled, image-intensified, and gated CCD detector (Instaspec V ICCD, Andor Technology, Belfast, Northern Ireland) having 1024 × 128 pixels. In front of the entrance slit, a cutoff filter (GG420, Schott, Mainz, Germany) was placed to prevent any elastically backscattered light from reaching the detector.

To increase the signal-to-noise ratio, the fluorescence from 20 pulses was added for each point measured. Every such measurement took ~ 2 s. For intensity reference, the peak maximum (at ~ 580 nm) of a fluorescence standard (10 mg Rhodamine 6G dissolved in 60 ml ethylene glycol) was recorded in connection with every measurement occasion. To measure the spectral response of the systems and providing a spectral correction, a spectrum of a calibrated blackbody radiation source was recovered.

Treatment System and Study Design

The therapeutic light source was a 2 W continuous-wave diode laser (Ceralas™ PDT 635, CeramOptec, Bonn, Germany) operating at a wavelength of 635 nm. The light-delivering system used consisted of the laser described above and a beam-splitting unit.[14] An optical fiber with a core diameter of 400 μm (Anda

KP-400L, Anda Optec, Livani, Latvia) was used to couple the light from the laser into the beam-splitting unit. Here, the light was divided into three or six different beams via a setup of beam splitters and different lenses. At the end of each pathway, the light was focused into a treatment fiber (Anda KP-400L, Anda Optec, Livani, Latvia). A multifiber arrangement was utilized with either three or six fibers (eight and four lesions, respectively) to deliver the therapeutic light to the patient. These fibers were placed in gentle contact with the treatment area. The total output through all treatment fibers ranged between 510 and 645 mW, whereas the maximum output from a single fiber was 215 mW. An aluminum ring with drilled holes for separate mounting of fiber holders was used to position the fibers (Fig. 1B). After each treatment the fibers were wiped off with aseptic cotton swabs and placed in Korsolex® basic 2% (Bode Chemie GmbH & Co, Hamburg, Germany) for a minimum of 4 hr for sterilization.

The treatment fibers were used to transmit the laser light onto the tumor, but can also act as receivers to measure the light fluence rate at the fiber tip. When the fluence rate was measured, a photodiode was switched into the pathway (at the position where the laser light normally was focused onto the fiber), preventing the laser light from that fiber to reach the tumor. This allowed the photodiode to detect the light from the other fibers, reaching the position of the fiber tip. These signals were separately calibrated to the fluence rate by placing the fibers into a tank with an Intralipid®/ink standard (Kabi Fresenius, Stockholm, Sweden and 05751 Ekströms Grön, Procordia Food AB, Kumla, Sweden, respectively) with known optical properties.

A custom-made program based on LabVIEW™ (National Instruments, Austin, TX) and C++™ (Microsoft Corporation, Seattle, WA) was used to control the light-delivery system. In the first part of the program, the operator defines the treatment setup (i.e., the shape and size of the tumor, absorption coefficients, and reduced scattering coefficients of the tumor and the healthy surrounding tissue). Then the fiber positions could be either manually selected, or the computer could calculate the optimal position by minimizing the total delivered light dose needed for complete treatment. This was done by numerically solving the diffusion equation[19] using finite element method calculations. The system also calculated the light dose in the different parts of the tissue. The threshold dose given to any part of the tumor was set to 30 J/cm^3, while at the same time minimizing the dose given to the healthy surrounding tissue.

In the second part of the program, the operator was guided through a few steps before and during the actual treatment. Issues for the operator interactions are where to position the fibers, when to turn the laser on, etc. During the treatment, a frequently updated image shows how much light has been delivered to the different parts of the tumor. The image also marks in false colors where the predefined tumor threshold dose has been reached. This information serves only as a guide to the treatment (because the computed map is based on calculations from the setup of the treatment). The treatment was interrupted every 30 s, and the fluence rate was measured at the fiber tips. Each measurement lasted for ~ 20 s. These measurements reveal if the optical properties have changed during the treatment. If so, this suggests that the treatment time should be al-

Table 1. Patient Data and Clinical Evaluation

Patient data				Follow-up treatment results						
					Visual evaluation					
					Clinical outcome			Cosmetic outcome		
Patient #	Age	Gender	Tumor location	Histological Outcome	1 month	7 months	28 months	1 month	7 months	28 months
1	69	F	Back	-	-	CR	CR	-	Excellent	Excellent
2	70	M	Back	CR	CR	-	CR	Good	-	Excellent[a]
3	70	M	Back	CR	CR	CR	CR	Good	Good	Good[b]
4	73	F	Back	CR	CR	CR	CR	Excellent	Excellent	Excellent
5	65	F	Thorax	CR	CR	CR	CR	Good	Excellent	Excellent
6	29	F	Back	CR	CR	CR	CR	Good	Excellent	Excellent
7	48	F	Trunk	CR	CR	CR	CR	Acceptable[c]	Acceptable[c]	Excellent
8	79	M	Back	[d]	[d]	[d]	[d]	[d]	[d]	[d]
9	79	F	Back	CR	CR	CR	CR	Good	Excellent	Excellent
10	77	M	Face	CR	CR	CR	CR	Good[e]	Good[e]	Good[e]
10	77	M	Back	PR[g]	PR[g]	PR[f,g]	CR	Good	Good	Excellent
10	77	M	Back	PR	PR	PR[f]	CR	Good	Good	Excellent

[a] Patient deceased from heart disease, evaluated at 26 months
[b] Fibrosis
[c] Hyperpigmented
[d] No show for follow-up
[e] Hypopigmented
[f] Punch excision due to the PR
[g] Insufficient treatment due to technical reasons

tered to fulfill the criteria of treatment. The calculated dose buildup in a particular treatment case is illustrated in Fig. 2. A more detailed description of the equipment and methods used can be found in Ref. 14.

Results

Clinical Outcome

The results of the treatments are included for each treated tumor in Table 1. At 1 month after the treatment, all but two patients returned for histological and visual assessment. Eight out of ten inspected tumors (80%) showed a complete response, whereas the two remaining showed partial response.

Tumor and treatment data for the 12 lesions are given in Table 2. The treatment times ranged from 4 min up to 30 min (for fully treated patients, see note *a* in Table 2), and the difference in delivered light dose was substantial. The reason for the large integrated dose delivered is the requirement that the outermost parts of the tumor, say point A in the right part of Fig. 1A, must be irradiated by a sufficient number of photons

Table 2. Tumor and Treatment Data

Tumor data			Treatment data			
Patient No.	Size (mm)	Thickness (mm)	Fibers used 3	Fibers used 6	Total output power (W)	Total delivered energy (J)
1	7 × 8	2–3	X		0.511	372
2	12 × 16	2–3	X		0.510	918
3	9 × 11	2–3	X		0.535	931
4	15 × 15	2–3		X	0.635	248
5	20 × 25	2		X	0.645	1152
6	12 × 12	2	X		0.545	883
7	11 × 15	2		X	0.594	270
8	9 × 12	2		X	0.634	274
9	9 × 9	2–3	X		0.59	334
10	5 × 7	6–7	X		0.59	684
10	6 × 6	3–4	X		0.59	71[a]
10	5 × 5	4–5	X		0.59	288

[a] Insufficient treatment because of technical reasons

from the fiber tips. These are positioned at a considerable distance away from these external tumor parts.

Seven months after the treatment, the patients (except for two individuals) returned to the Oncology Centre for clinical assessment. Again, eight out of ten evaluated tumors (80%) treated by MFC-PDT showed a complete response, whereas the two remaining (the same ones as at the one-month follow-up) showed a partial response. All lesions were biopsied at this follow-up to allow a better judgment and to ensure that the lesions were treated to the full thickness. At

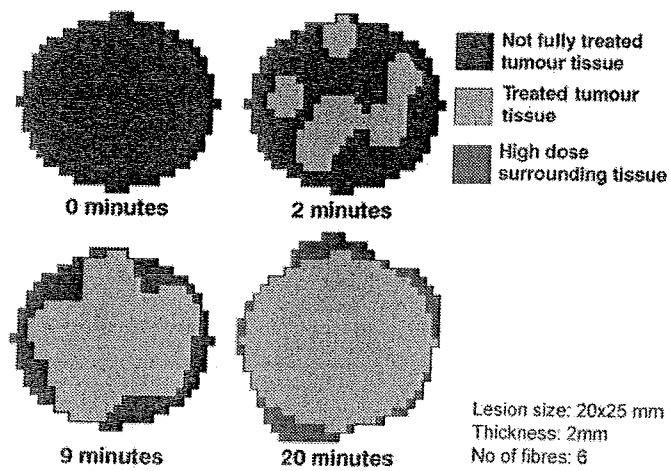

FIGURE 2 The buildup of delivered light dose at a 1 mm for patient number 5. As a threshold dose for full treatment, a total absorbed dose of 30 J/cm^3 was used.

the final follow-up, 11 tumors were examined; one patient (one lesion) consistently failed to appear at all the follow-up examinations. Two of the examined lesions with PR at the seven-month follow-up had, at the final follow-up, been converted to CR by the radical punch biopsy. For these two lesions the biopsy showed a minor, clearly delineated lesion. Thus, all tumors following the treatment protocol showed a complete response at this follow-up.

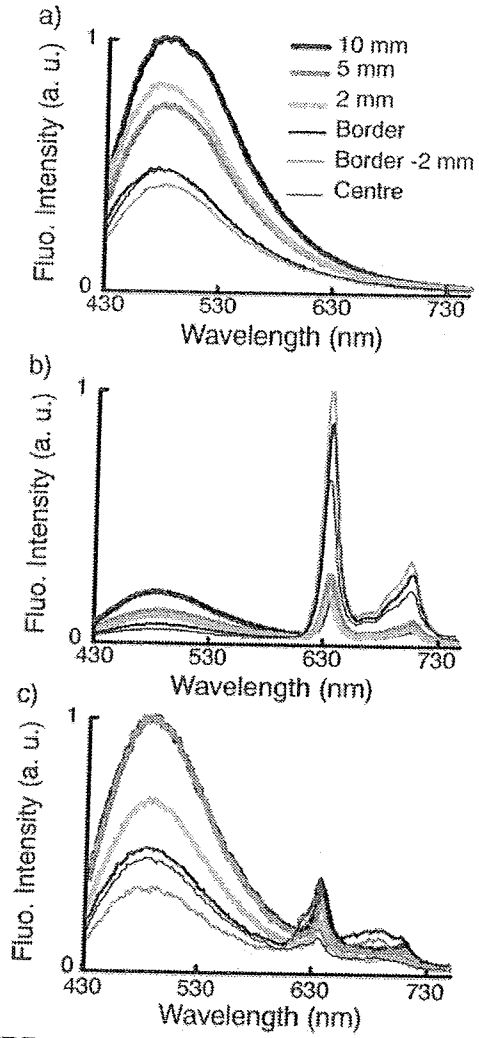

FIGURE 3 Case study of the geometrical variation of the fluorescence spectra of the skin **(A)** before applying the ALA cream, **(B)** before PDT; 6h after ALA cream application, and **(C)** after the therapeutic light delivery. In all of the figures above the measured sites were: 10, 5, and 2 mm outside the visible tumor border, at the tumor border, 2 mm inside the tumor border, and at the tumor center. Every spectrum is the mean value of three independent measurements at the same distance to the tumor border.

The cosmetic outcome was also evaluated at the 1-, 7-, and 28-month follow-up occasions. At the latter, more relevant evaluation, 82% (9/11) of the treated tumors showed an excellent cosmetic outcome. Also, poor healing due to any excess heat delivery to the tissue could not be seen in any of the lesions.

Diagnostic Measurements

Typical fluorescence data are displayed in Fig. 3. Recordings at different locations with regard to the tumor extension, as described above, are shown. The expected observation of a blue fluorescence reduction in the tumor area is verified in the upper part of the figure, pertaining to the time before ALA application.[16] Immediately before the PDT treatment (6 hr after ALA application), strong selective buildup of PpIX in the tumor area is illustrated in the middle part of the Fig. 3. Finally, almost complete PpIX bleaching is evident all through the investigated area after treatment. Bleaching is even evident at 10 mm outside the visible tumor border. Also in Fig. 3, the fluorescence data have been normalized to the highest value of each measurement series.

Figure 4A shows the bleaching of the PpIX during a tumor treatment, employing the multifiber contact PDT mode. The individual curves are recorded at asimilar location just inside the tumor border and corresponding to a location such as A indicated in Fig. 1A. This recording and the evaluated

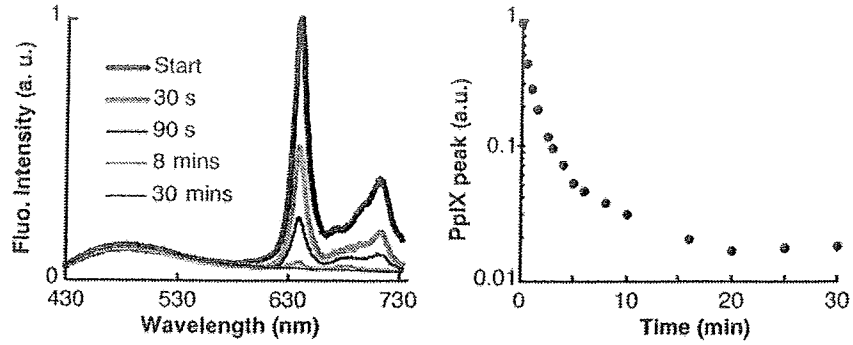

FIGURE 4 (A) Temporal evolution of the skin fluorescence at a given location during multifiber contact PDT. At each measurement occasion, the therapeutic light has been shut off. The different curves correspond to increasing irradiating times. **(B)** The fluorescence intensity at the 635 nm peak during the course of an MFC-PDT treatment.

bleaching data—the intensity of the 635 nm fluorescence peak—shown in Fig. 4B, clearly illustrate how the required dose is successively delivered to the outer tumor parts via diffusive light scattering.

Typical temporal evolution of the fluence rate during treatment is displayed in Fig. 5. In this figure, the measured light fluence rate from one fiber is measured in five other fibers. The distances between the illuminating fiber and the receiving fiber in Fig. 5 are between 5 and 11 mm. As can be seen, the fluence rate decreases slightly during the treatment.

Discussion and Conclusion

Even if the number of treated tumors is limited, the results of the MFC-PDT sessions are encouraging. For the modality employed, the efficacy as judged at a 7- and 28-month fol-

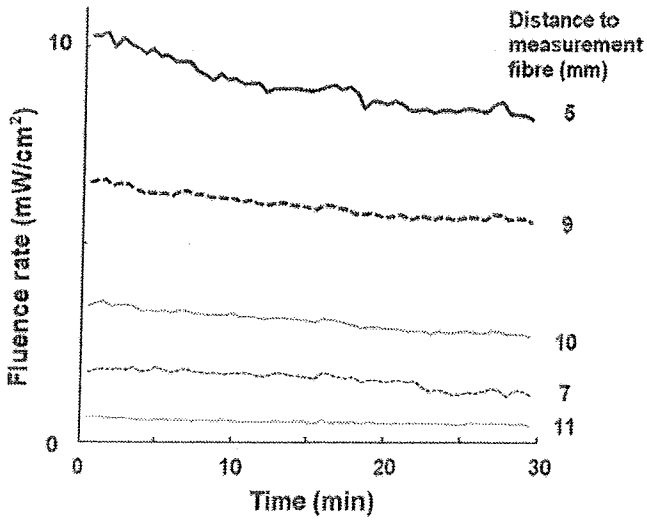

FIGURE 5 Typical recording of the fluence rate, as a function of time, during treatment. In this case one fiber serves as a light transmitter and five other fibers act as receivers.

low-up was 80% and 100% complete response, respectively. This is comparable to the results from several clinical trials for superficial PDT.[15,20,21] A plausible explanation for the cases of partial response at 7 months could be that these tumors were quite thick and in these cases ALA-PDT has previously proven not to be the treatment of choice, and additional treatment or preparation is required for efficient treatment.[22–25]

When comparing MFC-PDT to superficial PDT, two major issues need be addressed. First, there will be very high fluence rates centrally in the lesion, especially at the tip of the fibers, but also between closely positioned fibers because there will be an overlap of their corresponding light fluxes. The high total light dose given in MFC-PDT may be of importance for the successful treatment result in this study. The high fluence rate could, however, also lead to oxygen depletion or thermal damage close to the fiber tips and result in nonsatisfactory treatment. Second, one must assure that the boundary of the lesion has received enough light for proper treatment. None of these issues are critical in the same way when using conventional superficial PDT, since the light in this case can be considered to be uniformly distributed over the whole lesion area as well as some of the surrounding tissue (compare Fig. 1A). MFC-PDT, on the other hand, has the advantage of allowing direct feedback of the treatment by using the fibers both for light delivery and assessment of parameters of importance for the treatment. These aspects will be implemented in future work.

The comparable and good cosmetic outcome with this modality indicates that there is no permanent thermal damage due to any excess heating. The fluence rate at the tip of a 400 μm fiber delivering 215 mW (the maximum value in this study) is 171 W/cm^2. This value is several magnitudes higher than the values reported in other clinical trials.[17,26] Although very high fluence rates are obtained at the very tip of the treatment fibers this, as such, did not produce any discomfort to the patient.

The relatively low heating of the treatment volume is directly related to the low absorption and fairly low scattering (μ_a = 0.033 mm^{-1}, μ_s' = 2.73 mm^{-1}) of the treatment light in human skin.[27] This may be compared to canine prostate (μ_a = 0.073 mm^{-1}, μ_s' = 4.89 mm^{-1}),[28] where similar experimental studies resulted in substantial thermal damage when 300 mW at a wavelength of 630 nm was delivered through 600 μm fibers.[22] Furthermore, in the case of thicker and/or embedded tumors, the cosmetic results of the volume closest to the fiber tip is less critical because this region is generally diseased or necrotic and is, therefore, of moderate therapeutic and cosmetic importance. The fluence rates in these cases could then well exceed the levels in this study without restraining the treatment. Moreover, the efficient PpIX bleaching in the central parts would imply that the treatment is effectively self-terminating. Instead, the selective uptake of the drug in the tumor becomes the factor of major importance. Recent data on photobleaching of PpIX in solution[29] suggest that bleaching only occurs in the presence of oxygen, which means that there is no global depletion of the oxygen. That enough light really reached the boundary areas of the lesions is evidenced by the strong bleaching of the PpIX, as recorded by laser-induced fluorescence. Thus two potential problems with MFC-PDT were shown to be absent, and there is no obvious reason why this should be different in IPDT.

Studies have shown the total light dose cannot easily be correlated to the treatment result.[30] Although the PpIX is photobleached by reactive oxygen species, which also induce the tumor destruction in ALA-PDT, it would seem likely that they would correlate. Recent studies[31] show that it is rather the initial shift in reciprocal fluorescence that seems to predict the outcome, but the mechanism behind this has not yet been confirmed.

Since the treatment light is delivered in fractions of 30 s followed by a 20 s measurement session, it is possible that this might contribute to the good result of the study. Several studies have shown that fractionation leads to increased necrosis in PDT,[32–36] although the effect is lowered or not seen at all if the first fraction of the light is too large.[37,38]. The current explanation as to why fractionation might work is that the treated area is allowed to regain (approximately minutes) the oxygenation lost due the treatment or to reenable the buildup of the sensitizer (approximately hours). Thus the fractionation is of the magnitude enough to enable some reperfusion[32] of the treatment volume although too short to enable resynthesis of PpIX. Another recently suggested explanation[39] to the effect of fractionation is that the treatment increases the ratio of deoxyhemoglobin to hemoglobin. Since deoxyhemoglobin is more absorbing than hemoglobin at 635 nm, this will effectively reduce the penetration of the therapeutic light. The data shown in Fig. 5 could support this hypothesis because there is a decrease, although small, of the fluence rate during the treatment. This, on the other hand, would suggest that there is no effect of fractionation during our treatments, since the levels of light do not recover between measurements.

The main benefit of MFC-PDT compared to conventional superficial PDT is the possibility of monitoring the treatment by on-line dosimetry of several parameters; a feature that will now be implemented. The treatment methods do not differ in the actual treatment depth. However, there is a better coupling of the treatment light into the tissue because of a lower reflection between the fiber-tissue boundary as compared to the air-tissue boundary in the conventional case (due to the better matching of refractive indexes).[40–42]

Acknowledgments

This work was supported by the European Commission under the EU-IHP Access to Research Infrastructures Programme (Contract No. HPRI-CT-1999-00041), the Swedish Strategic Research Foundation, and the Swedish Institute (Visby Programme).

References

1. Kennedy JC, Pottier RH, Pross DC. Photodynamic therapy with endogenous protoporphyrin IX: Basic principles and present clinical experience. J Photochem Photobiol B 1990; 6:143–148.
2. Svanberg K, Andersson T, Killander D, Wang I, Stenram U, Andersson-Engels S, Berg R, Johansson J, Svanberg S. Photodynamic therapy of non-melanoma malignant tumours of the skin using topical δ-amino levulinic acid sensitization and laser irradiation. Br J Dermatol 1994; 130:743–751.
3. Peng Q, Warloe T, Berg K, Moan J, Kongshaug M, Giercksky K-E, Nesland JM. 5-aminolevulinic acid-based photodynamic therapy: Clinical research and future challenges. Cancer 1997; 79:2282–2308.

4. Zeitouni NC, Oseroff AR, Shieh S. Photodynamic therapy for nonmelanoma skin cancers: Current review and update. Mol Immunol 2003; 39(17–18):1133–1136.
5. Star WM. Light dosimetry *in vivo*. Phys Med Biol 1997; 42:763–787.
6. Svaasand LO, Wyss P, Wyss MT, Tadir Y, Tromberg BJ, Berns MW. Dosimetry model for photodynamic therapy with topically administered photosensitizers. Lasers Surg Med 1996; 18:139–149.
7. Calzavara-Pinton PG. Repetitive photodynamic therapy with topical δ-aminolaevulinic acid as an appropriate approach to the routine treatment of superficial nonmelanoma skin tumours. J Photochem Photobiol B 1995; 29(1):53–57.
8. Lowdell CP, Ash DV, Driver I, Brown SB. Interstitial photodynamic therapy. Clinical experience with diffusing fibres in the treatment of cutaneous and subcutaneous tumours. Br J Cancer 1993; 67:1398–1403.
9. Dougherty TJ, Thoma RE, Boyle DG, Weishaupt KR. Interstitial photoradiation therapy for primary solid tumors in pet cats and dogs. Cancer Res 1981; 41:401–404.
10. Marijnissen JPA, Versteeg JAC, Star WM, van Putten WLJ. Tumor and normal response to interstitial photodynamic therapy of the rat R-1 rhabdomyosarcoma. Int J Radiat Oncol Biol Phys 1992; 22:963–972.
11. Purkiss SF, Dean R, Allardice JT, Grahn M, Williams NS. An interstitial light delivery system for photodynamic therapy within the liver. Lasers Med Sci 1993; 8:253–257.
12. Chang SC, Buonaccorsi GA, MacRobert AJ, Bown S. Interstitial photodynamic therapy in the canine prostate with disulfonated aluminum phthalocyanine and 5-aminolevulinic acid-induced protoporphyrin IX. Prostate 1997; 32(2):89–98.
13. Bown SG, Rogowska AZ, Whitelaw DE, Lees WR, Lovat LB, Ripley P, Jones L, Wyld P, Gillams A, Hatfield AW. Photodynamic therapy for cancer of the pancreas. Gut 2002; 50(4):549–557.
14. Johansson T, Soto Thompson M, Stenberg M, af Klinteberg C, Andersson-Engels S, Svanberg S, Svanberg K. Feasibility study of a novel system for combined light dosimetry and interstitial photodynamic treatment of massive tumors. Appl Opt 2002; 41(7):1462–1468.
15. Wang I, Bendsoe N, af Klinteberg C, Enejder AMK, Andersson-Engels S, Svanberg S, Svanberg K. Photodynamic therapy versus cryosurgery of basal cell carcinomas; results of a phase III randomized clinical trial. Br J Dermatol 2001; 144(4):832–840.
16. af Klinteberg C, Enejder AMK, Wang I, Andersson-Engels S, Svanberg S, Svanberg K. Kinetic fluorescence studies of 5-aminolaevulinic acid-induced protoporphyrin IX accumulation in basal cell carcinomas. J Photochem Photobiol B 1999; 49(2–3): 120–128.
17. Soto Thompson M, Gustafsson L, Pålsson S, Bendsoe N, Stenberg M, af Klinteberg C, Andersson-Engels S, Svanberg K. Photodynamic therapy and diagnostic measurements of basal cell carcinomas using esterified and non-esterified δ-aminolevulinic acid. J Porphyrins Phthalocyanines 2001; 5(2):147–153.
18. af Klinteberg C, Andreasson M, Sandström O, Andersson-Engels S, Svanberg S. Compact medical fluorosensor for minimally invasive tissue characterisation. Rev Sci Instrum 2005; 76:034303-1-6.
19. Star WM. Diffusion theory of light transport. In: Welch AJ, van Gemert MJC, editors. Optical-Thermal Response of Laser-Irradiated Tissue. New York: Plenum Press, 1995, 131–206.
20. Soler AM, Warloe T, Berner A, Giercksky KE. A follow-up study of recurrence and cosmesis in completely responding superficial and nodular basal cell carcinomas treated with methyl 5-aminolaevulinate-based photodynamic therapy alone and with prior curettage. Br J Dermatol 2001; 145(3):467–471.

21. Morton CA, Mackie RM, Whitehurst C, Moore JV, McColl JH. Photodynamic therapy for basal cell carcinoma: effect of tumor thickness and duration of photosensitizer application on response. Arch Dermatol 1998; 134(2):248–249.
22. Peng Q, Warloe T, Moan J, Heyerdahl H, Steen HB, Nesland JM, Giercksky K-E. Distribution of 5-aminolevulinic acid-induced porphyrins in noduloulcerative basal cell carcinoma. Photochem Photobiol 1995; 62(5):906–913.
23. Fink-Puches R, Soyer HP, Hofer A, Kerl H, Wolf P. Long-term follow-up and histological changes of superficial nonmelanoma skin cancers treated with topical δ-aminolevulinic acid photodynamic therapy. Arch Dermatol 1998; 134(2):821–826.
24. Thissen MRTM, Schroeter CA, Neumann HAM. Photodynamic therapy with delta-aminolaevulinic acid for nodular basal cell carcinomas using a prior debulking technique. Br J Dermatol 2000; 142(2):338–339.
25. Haller JC, Cairnduff F, Slack G, Schofield J, Whitehurst C, Tunstall R, Brown SB, Roberts DJH. Routine double treatments of superficial basal cell carcinomas using aminolaevulinic acid-based photodynamic therapy. Br J Dermatol 2000; 143(6):1270–1275.
26. Svaasand LO. Photodynamic and photohyperthermic response of malignant tumors. Med Phys 1985; 12(4):455–461.
27. Simpson CR, Kohl M, Essenpreis M, Cope M. Near-infrared optical properties of ex vivo human skin and subcutaneous tissues measured using the Monte Carlo inversion technique. Phys Med Biol 1998; 43(9):2465–2478.
28. Nau WH, Roselli RJ, Milam DF. Measurement of thermal effects on the optical properties of prostate tissue at wavelengths of 1,064 and 633 nm. Lasers Surg Med 2003; 24(1):38–47.
29. Ericson MB, Grapengiesser S, Gudmundson F, Wennberg AM, Larkö O, Moan J, Rosén A. A spectroscopic study of the photobleaching of protoporphyrin IX in solution. Lasers Med Sci 2003; 18(1):56–62.
30. Robinson DJ, de Bruijn HS, van der Veen N, Stringer MR, Brown SB, Star WM. Fluorescence photobleaching of ALA-induced protoporphyrin IX during photodynamic therapy of normal hairless mouse skin: The effect of light dose and irradiance and the resulting biological effect. Photochem Photobiol 1998; 67(1):140–149.
31. Boere IA, Robinson DJ, de Bruijn HS, van den Boogert J, Tilanus HW, Sterenborg HJCM, de Bruin RWF. Monitoring in situ dosimetry and protoporphyrin IX fluorescence photobleaching in the normal rat esophagus during 5-Aminolevulinic acid photodynamic therapy. Photochem Photobiol 2003; 78(3):271–272.
32. Curnow A, McIlroy BW, Postle-Hacon MJ, MacRobert AJ, Bown SG. Light dose fractionation to enhance photodynamic therapy using 5-aminolevulinic acid in the normal rat colon. Photochem Photobiol 1999; 69(1):71–76.
33. Robinson DJ, de Bruijn HS, Wolf WJ, Sterenborg HJCM, Star WM. Topical 5-aminolevulinic acid-photodynamic therapy of hairless mouse skin using two-fold illumination schemes: PpIX fluorescence kinetics, photobleaching and biological effect. Photochem Photobiol 2000; 72(6):794–802.
34. Müller S, Walt H, Dobler-Girdziunaite D, Fiedler D, Haller U. Enhanced photodynamic effects using fractionated laser light. J Photochem Photobiol 1998; 42(1):67–70.
35. Robinson DJ, de Bruijn HS, Star WM, Sterenborg HJCM. Dose and timing of the first light fraction in two-fold illumination schemes for topical ALA-mediated photodynamic therapy of hairless mouse SkinP. Photochem Photobiol 2003; 77(3):319–323.
36. Thissen MR, de Blois MW, Robinson DJ, de Bruijn HS, Dutrieux RP, Star WM. PpIX Fluorescence kinetics and increased skin damage after intracutaneous injection of 5-

aminolevulinic acid and repeated illumination. J Invest Dermatol 2002; 118(2):239–245.
37. Robinson DJ, de Bruijn HS, Star WM, Sterenborg HJCM. Dose and timing of the first light fraction in two-fold illumination schemes for topical ALA-mediated photodynamic therapy of hairless mouse SkinP. Photochem Photobiol 2003; 77(3):319–323.
38. Babilas P, Schacht V, Liebsch G, Wolfbeis OS, Landthaler M, Szeimies R-M, Abels C. Effects of light fractionation and different fluence rates on photodynamic therapy with δ-aminolaevulinic acid *in vivo*. Br J Cancer 2003; 88(9):1462–1469.
39. Soumya M, Foster TH. Carbogen breathing significantly enhances the penetration of red light in murine tumours *in vivo*. Phys Med Biol 2004; 49(10):1891–1904.
40. Beuthan J, Minet O, Helfmann J, Herrig M, Müller G. The spatial variation of the refractive index in biological cells. Phys Med Biol 1996; 41(3):369–382.
41. Bolin FP, Preuss LE, Taylor RC, Ference RJ. Refractive index of some mammalian tissue using a fiber optic cladding method. Appl Opt 1989; 28(12):2297–2303.
42. Star WM, Wilson BC, Patterson MS. Light delivery and optical dosimetry in photodynamic therapy of solid tumors. In: Henderson BW, editor. Photodynamic Therapy. New York: Marcel Dekker, 1992; 335–367.

begell house, inc.
145 Madison Avenue, New York, NY 10016

JOURNAL OF ENVIRONMENTAL PATHOLOGY, TOXICOLOGY, AND ONCOLOGY

Special Issue: Photodynamic Therapy and Detection

Qian Peng, Guest Editor

Table of Contents

Volume 25, Issue 1-2, 2006

Editorial: Photodynamic Therapy and Detection 1
Biophysical Aspects of Photodynamic Therapy 7
Singlet Oxygen in Photosensitization 29
Hydrogen Peroxide, Superoxide, and Hydroxyl Radicals are Involved in the Phototoxic Action of Hematoporphyrin Derivative against Tumor Cells 51
Overview of Synthetic Approaches to Porphyrin, Phthalocyanine and Phenothiazine Photosensitisers for PhotoDynamic Therapy 79
New Derivatives of 5-Aminolevulinic Acid for Photodynamic Therapy: Chemical Synthesis and Porphyrin Production in In Vitro and In Vivo Biological Systems 109
Use of ALA and ALA Derivatives for Optimizing ALA-based Photodynamic Therapy: A Review of Our Experience 127
Regulation of Porphyrin Synthesis and Photodynamic Therapy in Heavy Metal Intoxication 145
Induction of Apoptosis by Hexaminolevulinate-Mediated Photodynamic Therapy in Human Colon Carcinoma Cell Line 320DM 159
Characterization of Apoptosis Induced by Photodynamic Treatment with Hypericin in A431 Human Epidermoid Carcinoma Cells 173
Deposition of Complement Proteins on Cells Treated by Photodynamic Therapy in Vitro 189
Photodynamic Effect of Curcumin on NPC/CNE2 Cells 205
Comparison of Merocyanine 540-Mediated Photodynamic Action on Leukemia Cells between Pulsed and Continuous Wave Light Sources 217
Perylenequinones in Photodynamic Therapy: Cellular versus Vascular Response 223
Positron Emission Tomography Imaging of Tumor Response after Photodynamic Therapy 239
Avastin Enhances Photodynamic Therapy Treatment of Kaposi's Sarcoma in a Mouse Tumor Model 251
Repetitive Photodynamic Therapy of Malignant Brain Tumors 261
Photoimmunotherapy for Cancer Treatment 281
Mechanism of Radiosensitization by Porphyrins 293
Spectroscopic Measurements of Photoinduced Processes in Human Skin after Topical Application of the Hexylester of 5-Aminolevulinic Acid 307
Methods for Detailed Histopathological Investigation and Localization of Biopsies from Cervix Uteri to Improve the Interpretation of Autofluorescence Data 321
Fluorescence Diagnosis Using Enzyme-Related Metabolic Abnormalities of Neoplasia 341
Updated Results of a Phase I Trial of Motexafin Lutetium-Mediated Interstitial Photodynamic Therapy in Patients with Locally Recurrent Prostate Cancer 373
Facilitated Delivery of ALA to Inaccessible Regions via Bioadhesive Patch Systems 389
Pretreatment of Plantar Warts with Azone Enhances the Effect of 5-Aminolevulinic Acid Photodynamic Therapy 403
Photodynamic Therapy of Nodular Basal Cell Carcinoma with Multifiber Contact Light Delivery 411
Fluorescence Diagnosis and Photodynamic Therapy in Dermatology: From Experimental State to Clinic Standard Methods 425
Photodynamic Applications in Superficial Bladder Cancer: Facts and Hopes! 441
Photodynamic Therapy and Detection of High-Grade Gliomas 453
PDT in Clinics: Indications, Results, Markets 467
Photodynamic Therapy as an Alternative Antimicrobial Modality for Oral Infections 487
Photodynamic Therapy of Microbial Infections: State of the Art and Perspectives 505
Photochemical Internalization (PCI): A New Modality for Light Activation of Endocytosed Therapeuticals 521

ISSN 0731-8998